



Design, synthesis, biological evaluation and molecular modeling of new coumarin derivatives as potent anticancer agents

Eman A. Fayed¹ · Rehab Sabour² · Marwa F. Harras² · Ahmed B. M. Mehany³

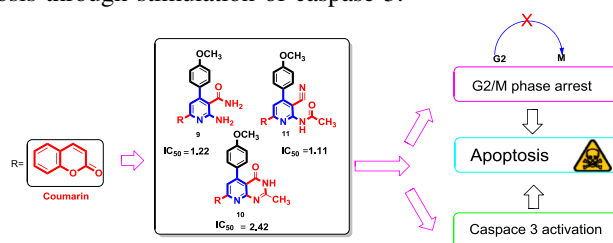
Received: 16 January 2019 / Accepted: 22 May 2019 / Published online: 1 June 2019
© Springer Science+Business Media, LLC, part of Springer Nature 2019

Abstract

A novel series of coumarin-pyridine/fused pyridine hybrids were designed and synthesized. Their anticancer activity was evaluated against human cancer cell lines MCF-7, HCT-116, HepG-2, and A549. Compounds **9**, **10**, and **11** showed the most potent growth inhibitory activities with IC₅₀ values ranging from 1.1 to 2.4 μM, against MCF-7 cell line. Flow cytometric analysis revealed that these compounds induced cell cycle arrest in the G2/M phase followed by apoptotic cell death. Consistent with these results, the activity of caspase-3 in MCF-7 cells was tested. The results indicated that compounds **9**, **10**, and **11** increased caspase-3 activity significantly compared to control group. Moreover, their binding affinity for caspase-3 was confirmed by docking study. Taking all these data together, it is suggested that these coumarin derivatives may be potential antiproliferative agents.

Graphical Abstract

One-pot synthesis of new coumarin derivatives: design, synthesis, molecular modeling and biological evaluation as potent anticancer agents. New coumarin hybrids were evaluated as antiproliferative agents, compounds **9**, **10** and **11** induced G2/M arrest and apoptosis through stimulation of caspase-3.



Keywords Coumarin-pyridine · Docking · Anticancer · Cell cycle and caspase-3 enzyme

Supplementary information The online version of this article (<https://doi.org/10.1007/s00044-019-02373-x>) contains supplementary material, which is available to authorized users.

- ✉ Eman A. Fayed
alfayed_e@yahoo.com
alfayed_e@azhar.edu.eg
- ✉ Marwa F. Harras
marwaharras.pharmg@azhar.edu.eg

- ¹ Pharmaceutical Organic Chemistry Department, Faculty of Pharmacy (Girls), Al-Azhar University, Cairo, Egypt
- ² Pharmaceutical Chemistry Department, Faculty of Pharmacy, Al-Azhar University (Girls), Cairo, Egypt
- ³ Department of Zoology, Faculty of Science (Boys), Al-Azhar University, Cairo, Egypt

Introduction

Cancer is considered as a main cause of death all over world (Juliana et al. 2011). It is described as uncontrolled growth of abnormal cells. Most of the anticancer drugs execute cancer cells by prompting apoptosis. Apoptosis is a controlled, selective, and genetically highly programmed cell death process arises as a result of normal cellular growth (Reed 2000). Coumarin is a bioactive scaffold of both natural and synthetic source and there has been a great interest in them owing to their diverse pharmaceutical activities (Salem et al. 2016). They are considered as attractive template for the development of potential anticancer agents (Vosooghi et al. 2010). Coumarin derivatives

Fig. 1 Structure of the lead anticancer coumarin derivatives

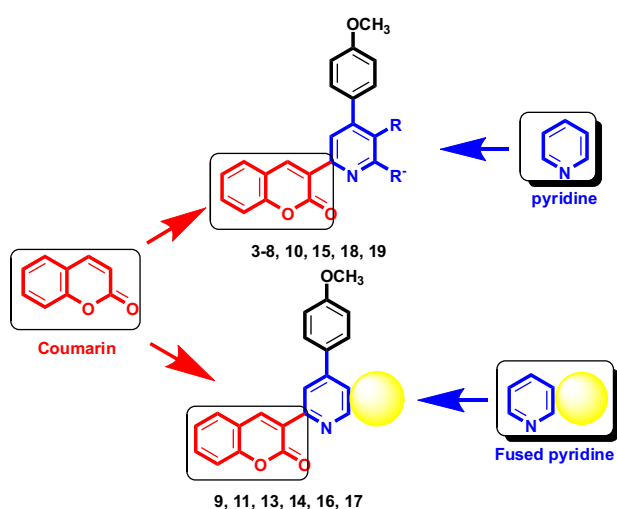
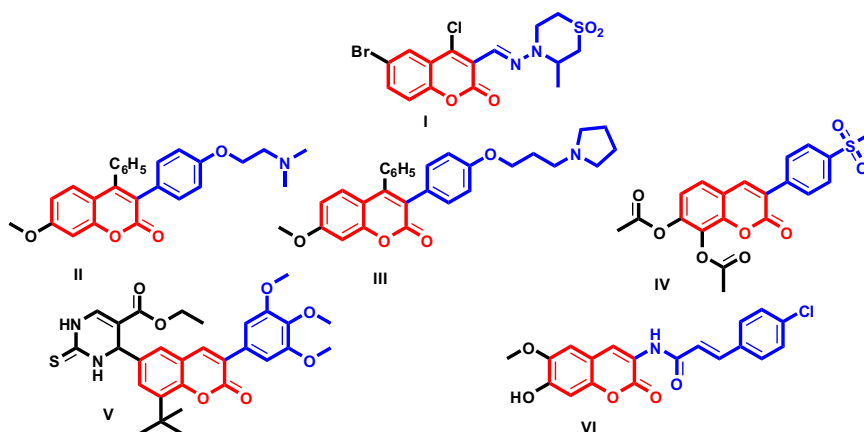


Fig. 2 Coumarin hybrids with pyridine and fused pyridine moieties

possess both cytostatic and cytotoxic properties as well (Benci et al. 2012). It has been reported that they inhibit growth in various human cancer cell lines (Marshall et al. 1994). Coumarins bearing different substitutions at 3-position are known to exhibit diverse biological activities including antitumor activity against ovarian carcinomas as compound **I** (RKS262) (Singh et al. 2011), against human lung cancer (A549) as compounds **II**, **III** (Musa et al. 2012) and **IV** (Musa et al. 2015). Moreover, compound **V** displayed potent cytotoxic effect against MCF-7. This compound induced apoptosis, caspase-3 activation and caused cell cycle arrest of MCF-7 at G1 phase (Sashidhara et al. 2013). Furthermore, SC-III3 (**VI**) showed effective cytotoxicity against HepG-2 (hepatocellular carcinoma) with high selectivity compared to the normal liver cell lines (Zhao et al. 2014). (Fig. 1)

Pyridines and fused pyridines are believed to possess a wide range of biological activities including antitumor effect (Nadia and Emad 2018). Currently there is a focus on

molecular hybridization to achieve a single biological architecture with high affinity and activity by joining two or more heterocyclic pharmacophores (Nagaraju et al. 2017; Nepali et al. 2014). The concept of hybridization is considered as a forward step in drug design to obtain a hybrid with improved pharmacokinetics and least side effects compared to the parent molecules. Therefore, hybrids of coumarin with a number of heterocyclic moieties have been reported to have biological importance as antiproliferative agents (Paul et al. 2013; Kini et al. 2012; Sashidhara et al. 2010).

In view of the former rationale and in continuation of our work to find novel structural leads with potent anticancer activities utilizing molecular hybridization, a new series of hybrids using coumarin and different pyridines or fused pyridine moieties have been designed (Fig. 2) and synthesized to evaluate their anticancer activities. A molecular docking study has also been carried out to support the effective binding of compounds at the active site of the target enzyme.

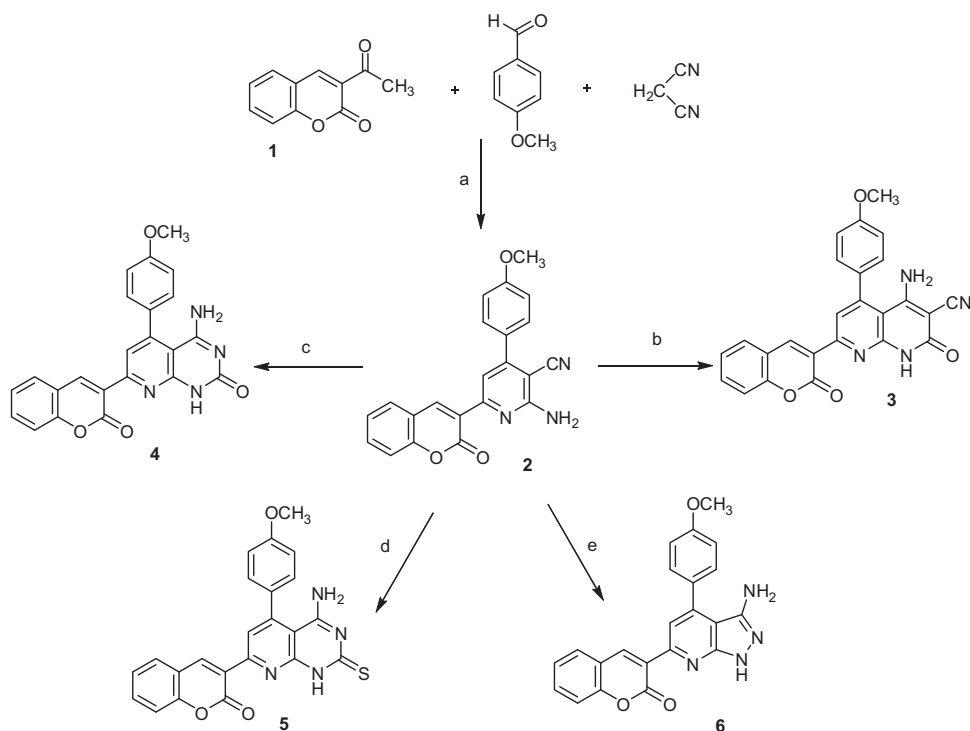
Results and discussion

Chemistry

The sequence of the reactions used in the synthesis of novel biologically active heterocyclic compounds is illustrated in Schemes 1–4. In this study we report a highly efficient method for the synthesis of a new series of pyridine and pyrimidine derivatives bearing coumarin moiety.

In Scheme 1, the key intermediate **2** was synthesized through one pot-synthesis reaction of compound **1**, 4-methoxybenzaldehyde and malononitrile in ammonium acetate and acetic acid. The compound **2** when subjected to heterocyclization with economically viable and easily available reagents such as, ethylcyanoacetate, urea, thiourea and hydrazine hydrate afforded compounds **3–6** in good

Scheme 1 Synthesis of compounds **2–6**. Reagents: **a** Amm. acetate, acetic acid, 6 h; **b** Ethyl cyanoacetate, Et₃N/EtOH, reflux 3 h; **c** Urea, EtOH, reflux 5 h; **d** Thiourea, EtOH, reflux 5 h; **e** NH₂NH₂·H₂O, EtOH, reflux 3 h



yields (Scheme 1). The synthesized compounds were characterized by elemental and spectral analyses.

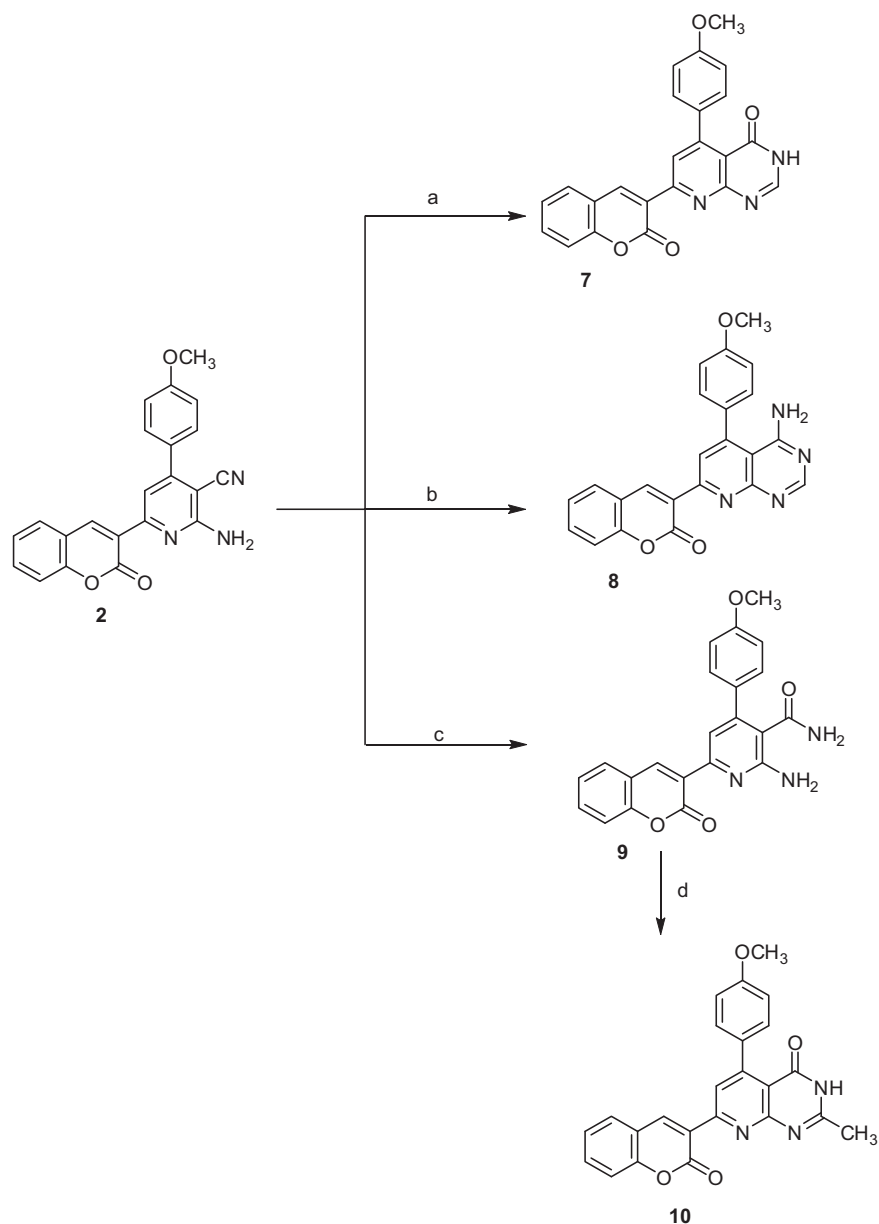
The starting material **2** was heated with formic acid to give compound **7**. The formation of compound **7** was assumed to proceed via the amide formation, followed by an intramolecular cyclization with formic acid to furnish the desired product (El-Gaby et al. 2006). The structure of **7** was confirmed with spectral data, where its IR spectrum showed bands at (ν , cm^{-1}) 3311 (NH) and 1710 and 1670 for C=O chromen and C=O amide, ¹H nuclear magnetic resonance (NMR) spectrum showed signals at δ 7.77 ppm for NH, which exchanged by D₂O. The mass spectrum of **7** represents a molecular ion peak at m/z 397 in addition to a base peak at 40. (Scheme 2)

On the other hand, the interaction of compound **2** with formamide when heated under reflux caused the formation of compound **8**. The latter compound was confirmed by spectral data and elemental analyses. Infrared (IR) spectrum represented an absorption band at (ν , cm^{-1}) 3393 for NH₂ and 1715 for C=O chromen in addition to the absence of cyano group. ¹H NMR, the appearance of a signal at δ 6.99 ppm for NH₂ which disappeared by D₂O. Furthermore, hydrolysis of **2** using 60% H₂SO₄ gave compound **9** in 86% yields. On cyclization using glacial acetic acid, compound **10** was produced. The formed new compounds were proved by spectral and elemental data for example, the absence of cyano group in IR and presence of 2 amino groups in **9** and only NH in **10** (Scheme 2).

In an attempt to synthesize compound **12** via condensation of compound **2** with triethyl-orthoformate in refluxing acetic anhydride was unsuccessful and compound **11** was obtained. Also, compound **11** was obtained through reaction of **2** with excess acetic anhydride when heated under reflux. On the other hand, acetylation of **2** using a 1:4 mixture of acetic anhydride and pyridine produced the *N,N*-diacetyl derivative **13** as greenish white crystals in 76% yield. Furthermore compound **2** was reacted with thioacetamide to produce compound **14** (Scheme 3).

Upon reaction of compound **2** with benzoyl chloride in pyridine when heated under reflux, compound **15** was obtained instead of compound **16**. The structure of **15** was confirmed by the disappearance of cyano group in IR spectra. The reaction of **2** with phenyl isothiocyanate in pyridine afforded compound **17** in good yield. The IR spectrum of compound **17** revealed the absorption bands at 3302, 1685, and 1250 for NH, C=O and C=S respectively. ¹H NMR for the same compound indicate an absorption band at δ 3.02 ppm for NH=C-CH-C=S and the ¹³C NMR showed an absorption at δ 180.05 ppm for C=S, in addition to the mass spectrum which represents a molecular ion peak at m/z 503 with a base peak at 408. Finally compound **18** was obtained through the reaction of **2** with carbon disulfide in dry pyridine through Dimroth Rearrangement (Scheme 4).

Scheme 2 Synthesis of compounds **7–10**. Reagent: **a** HCOOH, reflux, 6 h; **b** HCONH₂, reflux, 20 h; **c** 60% H₂SO₄, 30 min; **d** CH₃COOH, reflux 40 h



Antitumor properties

The in vitro cytotoxic activity of 14 new target compounds was evaluated against breast (MCF-7), colon (HCT-116), hepatocellular (HepG-2), and lung (A549) cancer cell lines. 5-Fluorouracil (5-FU), a well-known chemotherapeutic agent, was used as the reference drug. Bioactivities of the reference and target compounds were evaluated by MTT assay. The IC₅₀ values were calculated and listed in Table 1.

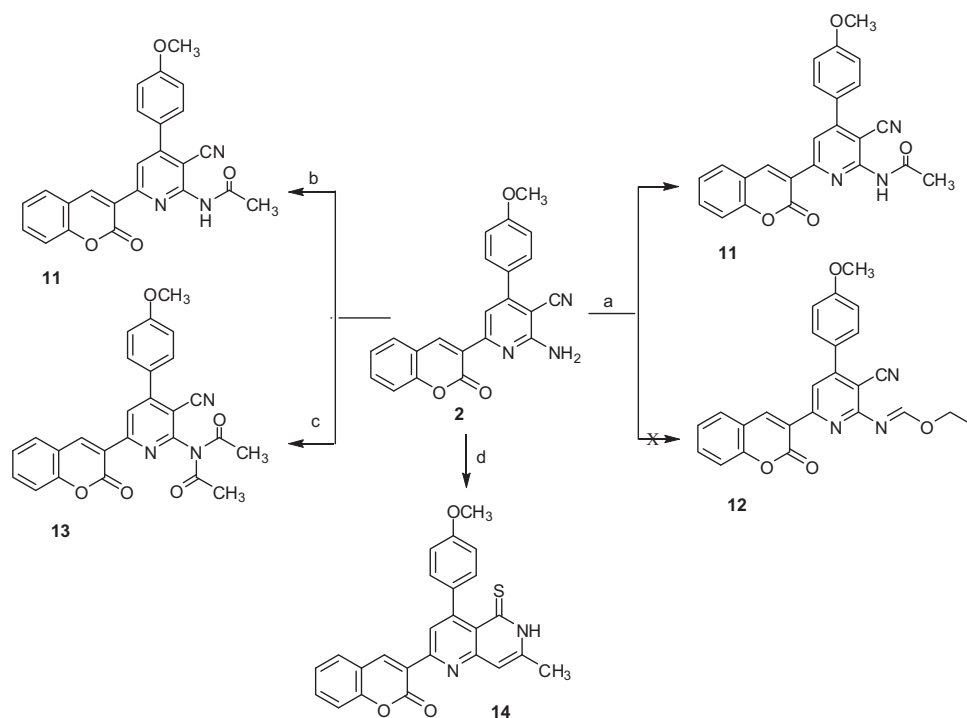
The anticancer profile suggested that test compounds showed variable activities compared to the reference drug. In general, compounds **8**, **9**, **10**, **11**, **13**, and **17** displayed significant anti-proliferative activity against most of the tested cell lines. Particularly, they were active against MCF-7 with

IC₅₀ values ranging from 1.11 to 4.55 μM and against HCT-116 with IC₅₀ values ranging from 5.14 to 8.75 μM comparing to 5-FU with IC₅₀ values (7.76 μM and 8.78 μM, respectively).

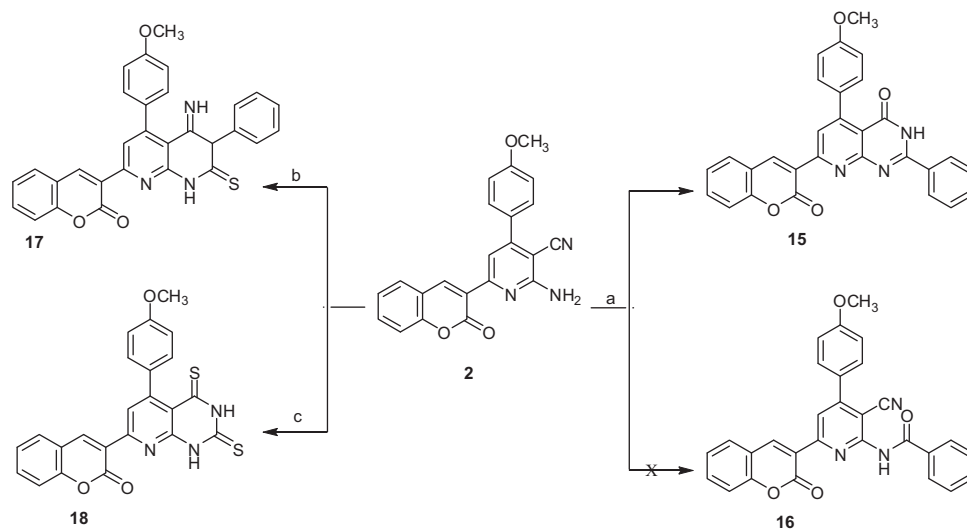
Concerning compounds having pyridine moiety at position 3 of the coumarin ring as in compounds **9**, **11**, and **13**, high anticancer activity was displayed against the tested cell lines. It was found that diacetyl derivative **13** displayed slightly decrease in the activity than the monoacetylated one **11**. Fusion of pyridine with five membered rings as in compound **6** resulted in a mild reduction in activity.

For coumarin compounds bearing pyridopyrimidine moiety at position 3, results revealed that substitution at position 2 and/or 4 in the pyridopyrimidine ring with C=O or C=S resulted in reduction in activity as in compounds **4**,

Scheme 3 Synthesis of compounds **11–14**. Reagents: **a** TEOF, AC₂O, reflux 3 h; **b** AC₂O, reflux, 5 h; **c** AC₂O, pyridine, reflux, 1 h; **d** CH₃CSNH₂, TFA, reflux, 24 h



Scheme 4 Synthesis of compounds **15–18**. Reagents: **a** B.C, Pyridine, reflux, 6 h; **b** PhNCS, Pyridine, reflux, 7 h; **c** CS₂, Pyridine, reflux (w.b.), 8 h



5, **7**, and **18** with exception of compound **10** bearing methyl group at position 2 and C=O at position 4, exhibited significant anticancer activity.

In case of coumarin derivatives having 1,8-naphthyridin ring at position 3, it was found that compound **3** has moderate activity against tested cell lines, while compound **17** showed high activity against MCF-7 and HCT-116 (4.22 μ M and 8.18 μ M, respectively).

However, for coumarins having 1,6-naphthyridin ring, compound **15** with C=S at positions 5 revealed higher cytotoxic activity than compound **13** bearing C=O group at the same position.

From our study, we noticed that the anticancer activity of our new compounds was promising especially against MCF-7 cell line.

Cell cycle analysis

Many cytotoxic compounds produce their anticancer activity by induction of apoptosis or by arresting the cell or a combined effect of both (Chan et al. 2010; Shen et al. 2009). Furthermore, apoptosis and cell cycle regulation are believed to be important strategies in the development of antitumor agents (Blank and Shiloh 2007). The anticancer

Table 1 Cytotoxicity of compounds **3–18** and 5-FU assessed in different human cancer cells

| Compounds | IC50 (µM) | | | |
|-------------|--------------|--------------|--------------|--------------|
| | MCF-7 | HCT-116 | HEPG-2 | A549 |
| 3 | 26.32 ± 1.01 | 15.42 ± 1.13 | 15.01 ± 1.3 | 14.72 ± 0.98 |
| 4 | 33.59 ± 2.25 | 27.12 ± 2.1 | 24.13 ± 2.23 | 31.83 ± 1.8 |
| 5 | 52.43 ± 3.45 | 32.47 ± 2.24 | 42.56 ± 1.58 | 33.11 ± 1.81 |
| 6 | 12.13 ± 1.13 | 14.78 ± 1.45 | 11.22 ± 0.53 | 16.24 ± 0.57 |
| 7 | 37.71 ± 1.35 | 31.25 ± 2.12 | 29.54 ± 1.45 | 27.94 ± 1.56 |
| 8 | 4.55 ± 0.61 | 5.48 ± 0.95 | 7.45 ± 0.52 | 6.86 ± 0.71 |
| 9 | 1.22 ± 0.41 | 5.14 ± 0.48 | 12.01 ± 0.58 | 15.25 ± 0.83 |
| 10 | 2.42 ± 0.75 | 6.11 ± 0.82 | 13.32 ± 0.41 | 17.21 ± 0.71 |
| 11 | 1.11 ± 0.28 | 6.44 ± 0.62 | 4.51 ± 0.78 | 7.18 ± 0.71 |
| 13 | 3.29 ± 0.35 | 8.75 ± 1.2 | 9.18 ± 1.1 | 7.46 ± 0.64 |
| 14 | 9.33 ± 1.15 | 7.74 ± 0.62 | 8.63 ± 1.1 | 7.06 ± 0.61 |
| 15 | 17.85 ± 1.65 | 24.75 ± 0.52 | 43.48 ± 1.41 | 38.45 ± 1.81 |
| 17 | 4.22 ± 0.51 | 8.18 ± 1.1 | 24.52 ± 1.9 | 18.96 ± 0.57 |
| 18 | 43.05 ± 2.35 | 28.02 ± 2.35 | 23.67 ± 2.65 | 19.48 ± 0.82 |
| 5-FU | 7.76 ± 0.46 | 8.78 ± 0.58 | 8.15 ± 0.61 | 7.65 ± 0.67 |

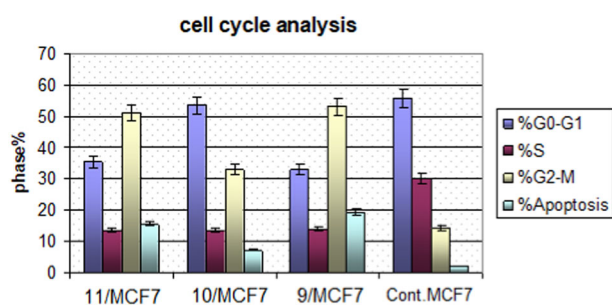


Fig. 3 Cell cycle analysis of MCF7 cells after treatment with compounds **9**, **10**, and **11** and DMSO controls

results showed that compounds **9**, **10**, and **11** have significant anticancer activity against MCF-7. Therefore, it is important to know if this cell growth inhibition was on account of cell cycle arrest. Cell cycle arrest flow cytometry analysis was done using propidium iodide (PI) staining of DNA where MCF-7 cells were incubated with IC₅₀ concentration of these compounds and their effect on the normal cell cycle profile was analyzed.

The results shown in Fig. 3 indicated a marked increase of DNA content in G2/M phase and subsequent reduction in G0/G1, and S phases in comparison to the control cells. Moreover, significant increase in the percentage of cells was observed at the pre-G phase. These results demonstrate that our compounds caused interference with the normal cell cycle distribution in breast carcinoma cell line as a result of G2/M phase arrest, followed by apoptotic cell death.

Table 2 Induction of apoptosis of MCF7 cells by **9**, **10**, and **11**

| Sample data | Apoptosis | | | % Necrosis |
|-------------------|-----------|---------|--------|------------|
| | %Total | % Early | % Late | |
| 9/MCF7 | 19.31 | 4.28 | 9.84 | 5.19 |
| 10/MCF7 | 7.27 | 1.87 | 3.21 | 2.19 |
| 11/MCF7 | 15.62 | 3.86 | 7.29 | 4.47 |
| Cont. MCF7 | 2.16 | 0.38 | 0.22 | 1.56 |

Apoptosis study

Programmed cell death, or apoptosis, is a highly regulated cellular process that takes place in physiological and pathological conditions, and is involved in tissue homeostasis. Disruption of different apoptotic pathways result in tumor cells overgrowth (Kamal et al. 2014; Fan et al. 2010).

Consequently, the induction of apoptosis is considered as a key approach in cancer treatment. Table 2 and Fig. 4 showed the effects of **9**, **10**, and **11** on the percentage of the apoptotic cells (both early and late stages) in MCF-7 cell line, the results showed that these compounds caused marked increase in percentage of the apoptotic MCF-7 cells and decrease in percentage of the viable tumor ones compared to the untreated samples, demonstrating that the tested compounds inhibited MCF-7 cells proliferation by induction of cytotoxicity and apoptosis.

Caspase-3 activity assay

The main characteristics of apoptosis is the activation various protease enzymes that are cysteine protease families

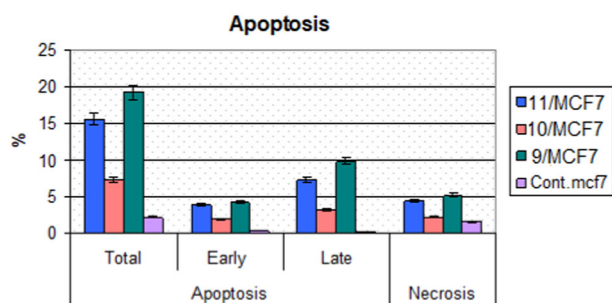


Fig. 4 The percentage of apoptosis and necrosis caused by compounds **9**, **10**, and **11** using MCF7 cell line

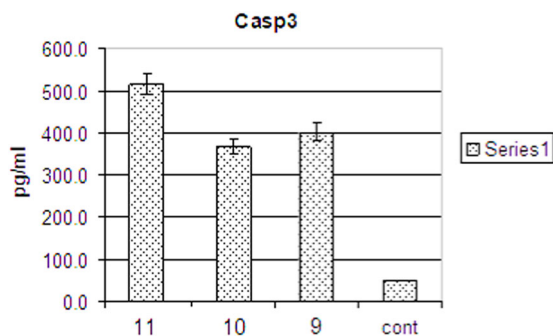


Fig. 5 A diagram illustrated the effect of compounds **9**, **10**, and **11** regarding apoptotic induction of Caspase-3

called caspases. Caspase-3, one of the key proteins of the caspase family, is the main target for a number of anticancer agents (Eissa 2017). The activity of caspase-3 in MCF-7 cells treated by **9**, **10**, and **11** was highly overexpressed (Fig. 5). Results revealed that compounds **9**, **10**, and **11** upregulated the level of active caspase-3 by 8.35, 7.54, and 10.73 folds, respectively as compared to the control, indicating that all three coumarin derivatives effectively induced MCF-7 cancer cell apoptosis.

Docking study

In order to gain more insight into the binding modes of our active compounds **9**, **10**, and **11** and caspase-3, docking study was done for them by using molecular operating environment (MOE) software (MOE 2008.10). The crystal structure of caspase-3 was downloaded from Protein Data Bank (PDB ID: 1GFV) (Lee et al. 2000). Docking study showed that compounds **9**, **10**, and **11** are able to fit in the binding pocket of caspase-3 with high binding energies, -7.115 , -6.224 , and -7.156 Kcal/mol, respectively.

Results revealed that the activator **9** is suitably situated at the binding site with various interactions between it and the binding region of the enzyme (Fig. 6). It formed three hydrogen bond interactions; two hydrogen bonds are

formed between the two amino groups and Ser120 while the third one is formed between the amide carbonyl oxygen and Arg207. Furthermore, arene–cation interaction is found between the phenyl ring and Arg207.

Similar to compound **9**, compound **10** was also docked at the same binding pockets (Fig. 7). Results showed that the oxygen atom of the pyridopyrimidinone moiety formed a hydrogen bond with Gly122 residue. Moreover, the nitrogen of the pyrimidine ring showed additional hydrogen bonding with Arg207. In addition, arene–arene interaction is seen between the chromene moiety and Phe256.

Whereas in compound **11**, three hydrogen bond interactions are observed as shown in Fig. 8; one between the nitrogen of the pyridine ring and His121, another hydrogen bond is formed between the carbonyl oxygen and Gly122, the third one is formed between the cyano nitrogen and Arg207.

Besides this, these compounds (**9**, **10**, and **11**) showed hydrophobic interactions with the target protein. The methoxyphenyl and the chromenone moieties are found in close contact with the hydrophobic pocket of the enzyme (Met61, His121, Glu123, Tyr204, Trp206, Arg207, and Phe256).

Conclusion

In this study, a novel series of coumarin hybrids were synthesized and evaluated for their cytotoxic activity against four human tumor cells (MCF-7, HCT-116, HepG-2, and A549) in comparison with 5-FU. Compounds **9**, **10**, and **11** showed potent and broad spectrum anticancer activity against the tested cell lines. Further biological assessments of **9**, **10**, and **11** indicated that these compounds cause cell cycle arrest at G2/M phase in MCF-7 cells. Moreover, they induced apoptosis through the stimulation of caspases-3. These results suggest that these compounds are promising lead molecules for further development of potent anticancer agents.

Experimental

Chemistry

All melting points were measured on an Electrothermal LA9000 series Digital melting point apparatus and were uncorrected. IR spectra were determined using the KBr disc technique on a Nicolet IR 200 FT-IR Spectrophotometer at the Pharmaceutical Analytical Unit, Faculty of Pharmacy, Al-Azhar University, Egypt, and values are represented in cm^{-1} . The ^1H NMR and ^{13}C NMR spectra were recorded on

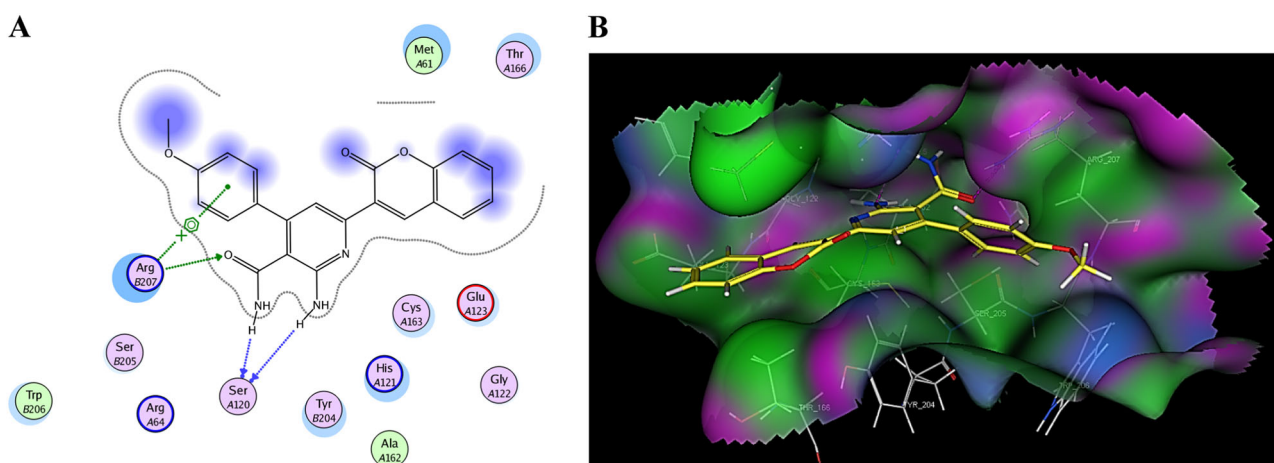


Fig. 6 The proposed binding mode of the **9** docked in the active site of Caspase-3; **a, b** 2D and 3D ligand-receptor interactions (hydrogen bonds are illustrated as arrows; C atoms are colored yellow, N blue and O red) (color figure online)

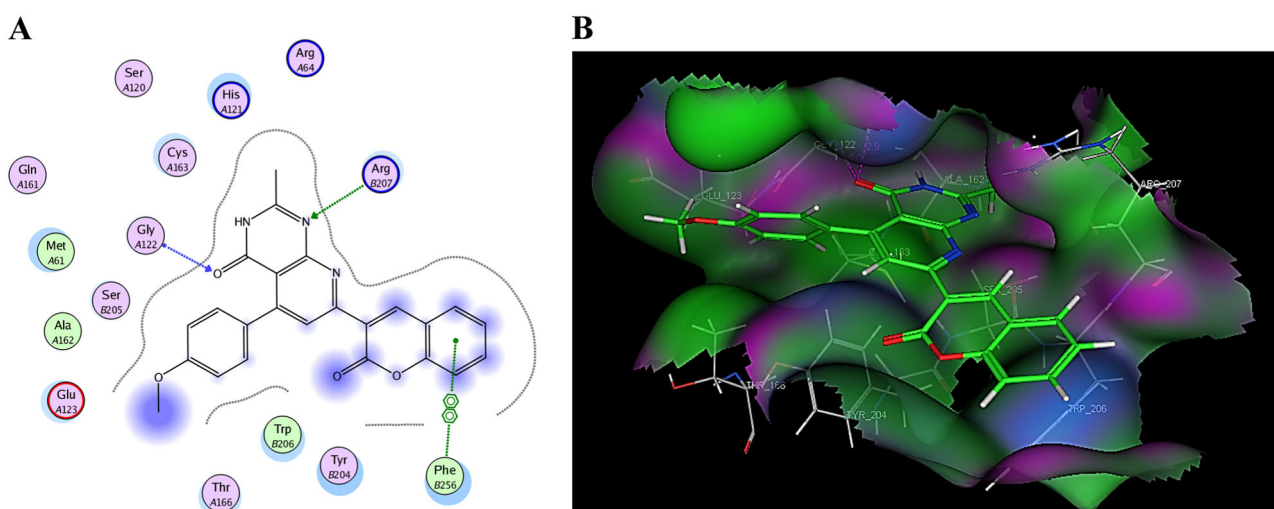


Fig. 7 The proposed binding mode of the **10** docked in the active site of Caspase-3; **a, b** 2D and 3D ligand-receptor interactions (hydrogen bonds are illustrated as arrows; C atoms are colored green, N blue and O red) (color figure online)

Gemini 400 MHz, and Mercury 100 MHz NMR Spectrometers at the Main Chemical Warfare Laboratories, Chemical Warfare Department, Ministry of Defense, Cairo, Egypt. Dimethyl sulfoxide (DMSO)- d_6 was used as solvent, and chemical shifts were measured in δ ppm, relative to TMS as an internal standard. Mass spectrum was recorded at 70 eV on a DI-50 unit of a Shimadzu GC/MS-QP5050A Spectrometer at the Regional Center for Mycology and Biotechnology (RCMB), at Al-Azhar University, represented as m/z (relative abundance %) (formula). Element analysis (C, H, N) were also carried out at Regional Center for Mycology and Biotechnology, and the values were found to be within $\pm 0.4\%$ of the theoretical ones unless otherwise indicated. The progress of the reaction was monitored by thin layer chromatography (TLC) using TLC

sheets pre-coated with UV fluorescent silica gel Merck 60 F254 plates and was visualized using a UV lamp.

Acetyl-2*H*-chromen-2-one 3-(1)

This compound was prepared according to reported method (Siddiqi et al. 2009).

2-Amino-4-(4-methoxyphenyl)-6-(2-oxo-2*H*-chromen-3-yl) nicotinonitrile (2)

A mixture of acetyl-2*H*-chromene-2-one 1 (10 mmol), active methylene namely malononitrile (10 mmol) and 4-methoxybenzaldehyde (10 mmol), were heated under reflux for 6 h in glacial acetic acid and ammonium acetate as

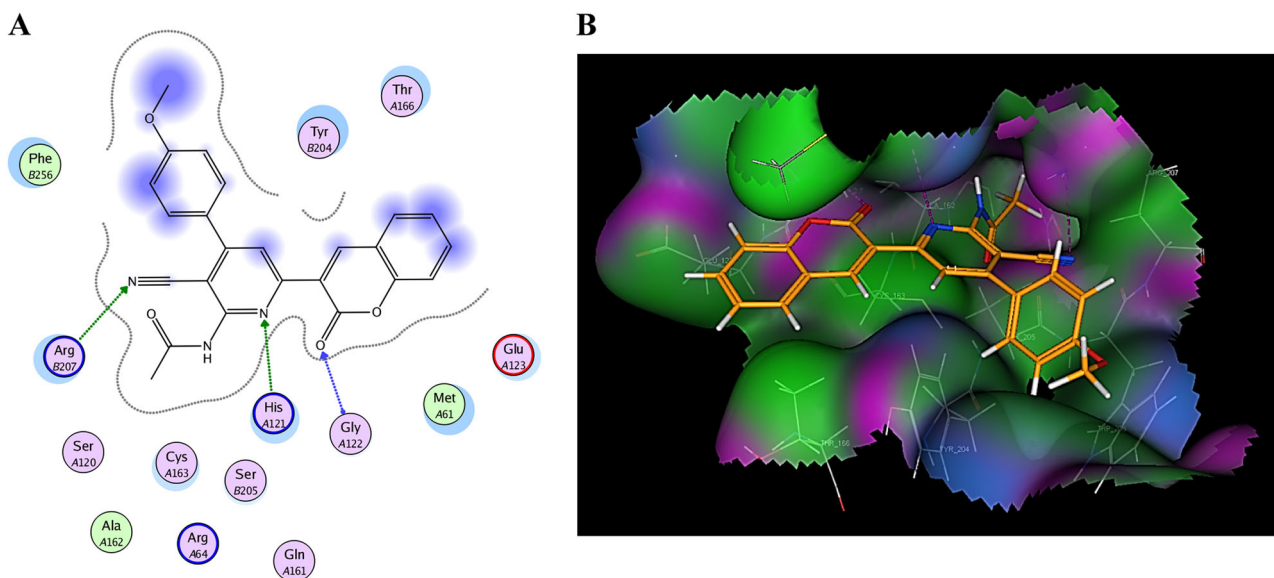


Fig. 8 The proposed binding mode of the **11** docked in the active site of Caspase-3; **a, b** 2D and 3D ligand-receptor interactions (hydrogen bonds are illustrated as arrows; C atoms are colored orange, N blue and O red) (color figure online)

catalyst. The reaction vessel was cooled to room temperature. The solid compound was collected by filtration, washed with water, and recrystallized from ethanol to give pure compound.

Yellow crystals; yield: 90%; m.p.: 79–81 °C; IR (KBr, cm^{-1}): 3349, 3242 (NH_2), 3081 (Ar–H), 2940, 2835 (aliph C–H), 2218 (CN), 1738 ($\text{C}=\text{O}$ chromen); ^1H NMR (400 MHz, DMSO-d_6): δ = 3.86 (s, 3H, OCH_3), 5.38 (s, 2H, NH_2 , exchangeable by D_2O), 7.09 (d, 2H, J = 8 Hz, Ar–H), 7.15 (d, 2H, J = 8 Hz, Ar–H), 7.83 (d, 2H, J = 8 Hz, Ar–H), 7.92 (t, 2H, Ar–H), 8.08 (s, 1H, H-pyridine); 8.36 (s, 1H, H-chromen); MS (EI, 70 eV): m/z (%) = 369 [M^{+}] (7.93), 277 (100).

4-Amino-5-(4-methoxyphenyl)-2-oxo-7-(2-oxo-2H-chromen-3-yl)-1,2-dihydro-1,8-naphthyridine-3-carbonitrile (**3**)

A mixture of compound **2** (10 mmol) and ethyl cyanoacetate (10 mmol) in ethyl alcohol (20 mL) in the presence of catalytic amount of triethylamine (Et_3N) was heated under reflux for 2 h. Then, the reaction mixture was poured onto ice-cold water (30 mL). The resulting solid was collected and crystallized from ethanol.

Yellow crystals; yield 850%; m.p.: 296–298 °C; IR (KBr, cm^{-1}): 3452 (br NH_2 and NH), 3101 (Ar–H), 2205 (CN), 1720–1624 (br. $2\text{C}=\text{O}$ chromen and amide); ^1H NMR (400 MHz, DMSO-d_6): δ = 3.79 (s, 3H, OCH_3), 4.32 (s, 2H, NH_2 , exchangeable by D_2O), 6.97 (s, 1H, H-Pyridine), 6.98 (d, 4H, J = 8 Hz, Ar–H), 7.31–7.93 (m, 5H, 4 Ar–H, and H-chromen), 10.47 (s, 1H, NH exchangeable by D_2O); ^{13}C NMR (100 MHz, DMSO-d_6): δ = 55.62 (OCH_3), 82.05, 110.00, 113.96, 119.48 (CN), 128.93, 129.89,

160.31, 162.07 (CO), 163.90 (CO); MS (EI, 70 eV): m/z (%) = 436 [M^{+}] (5.99), 377 (100); Anal. calcd for $\text{C}_{25}\text{H}_{16}\text{N}_4\text{O}_4$ (436.42): C, 68.80; H, 3.70; N, 12.84; Found: C, 69.12; H, 3.82; N, 13.11%.

4-Amino-5-(4-methoxyphenyl)-7-(2-oxo-2H-chromen-3-yl)pyrido[2,3-*d*]pyrimidin-2(1H)-one (**4**)

A mixture of compound **2** (10 mmol) and urea (10 mmol) in ethyl alcohol (20 mL) was heated under reflux for 5 h. Then, the reaction mixture was poured onto ice-cold water (30 mL). The resulting solid was collected and crystallized from ethanol.

Yellow crystals; yield 85%; m.p.: 120–122 °C; IR (KBr, cm^{-1}): 3446–3179 (br NH_2 and NH), 3050 (Ar–H), 1715–1660 ($\text{C}=\text{O}$ chromen and $\text{C}=\text{O}$ amide); ^1H NMR (400 MHz, DMSO-d_6): δ = 3.86 (s, 3H, OCH_3), 7.10 (s, 2H, NH_2 , exchangeable by D_2O), 7.12 (d, 2H, J = 8 Hz, Ar–H), 7.16 (d, 2H, J = 8 Hz, Ar–H), 7.93 (t, 2H, Ar–H), 7.97 (s, 1H, H-Pyridine), 8.09 (s, 1H, H-Pyridine), 8.38 (s, 2H, H-chromen and 1H, NH exchangeable by D_2O); ^{13}C NMR (100 MHz, DMSO-d_6): δ = 56.08 (OCH_3), 115.28 (CN), 115.69, 124.59, 132.90, 133.83, 150.59, 160.94 (2CO); MS (EI, 70 eV): m/z (%) = 412 [M^{+}] (3.59), 408 (100); Anal. calcd for $\text{C}_{23}\text{H}_{16}\text{N}_4\text{O}_4$ (412.40): C, 66.99; H, 3.91; N, 13.59; Found: C, 67.26; H, 3.82; N, 13.82%.

3-(4-Amino-5-(4-methoxyphenyl)-2-thioxo-1,2-dihydropyrido[2,3-*d*]pyrimidin-7-yl)-2H-chromen-2-one (**5**)

A mixture of compound **2** (10 mmol) and thiourea (10 mmol) in ethyl alcohol (20 mL) was heated under reflux

for 5 h. Then, the reaction mixture was poured onto ice-cold water (30 mL). The resulting solid was collected and crystallized from ethanol.

Yellow crystals; yield 87%; m.p.: 132–133 °C; IR (KBr, cm^{-1}): 3446–3315 (br NH and NH_2), 3180 (Ar–H), 1710–1699 (C=O chromen), 1263 (C=S); ^1H NMR (400 MHz, DMSO-d_6): δ = 3.91 (s, 3H, OCH_3), 4.12 (s, 1H, NH exchangeable by D_2O), 6.16 (s, 2H, NH_2 , exchangeable by D_2O), 6.55 (s, 1H, H-Pyridine), 6.96 (m, 8H, Ar–H), 8.98 (s, 1H, H-chromen); MS (EI, 70 eV): m/z (%) = 428 [M^{+}] (5.82), 336 (100); Anal. calcd for $\text{C}_{23}\text{H}_{16}\text{N}_4\text{O}_3\text{S}$ (428.46): C, 64.47; H, 3.76; N, 13.08; Found: C, 64.53; H, 3.94; N, 12.79%.

3-(3-Amino-4-(4-methoxyphenyl)-1H-pyrazolo[3,4-b]pyridin-6-yl)-2H-chromen-2-one (6)

A mixture of compound **2** (10 mmol) and hydrazine hydrate (20 mmol) in ethyl alcohol (20 mL) was heated under reflux for 3 h. The reaction mixture was cooled and poured onto ice-cold water (30 mL). The resulting solid deride, filtered and crystallized from methanol.

Yellow crystals; yield 62%; m.p.: 150–152 °C; IR (KBr, cm^{-1}): 3309–3213 (br NH and NH_2), 3066 (Ar–H), 1715 (C=O chromen); ^1H NMR (400 MHz, DMSO-d_6): δ = 3.81 (s, 3H, OCH_3), 6.52 (s, 2H, NH_2 , exchangeable by D_2O), 6.77 (d, 4H, J = 8 Hz, Ar–H), 6.85 (t, 2H, Ar–H), 6.56 (s, 1H, H-Pyridine), 7.04 (d, 2H, J = 8 Hz, Ar–H), 8.60 (s, 1H, H-Pyridine), 8.90 (s, 1H, NH exchangeable by D_2O); MS (EI, 70 eV): m/z (%) = 384 [M^{+}] (3.76), 111 (100); Anal. calcd for $\text{C}_{22}\text{H}_{16}\text{N}_4\text{O}_3$ (384.39): C, 68.74; H, 4.20; N, 14.58; Found: C, 69.02; H, 4.37; N, 14.25%.

5-(4-Methoxyphenyl)-7-(2-oxo-2H-chromen-3-yl)pyrido[2,3-d]pyrimidin-4(3H)-one (7)

A mixture of compound **2** (10 mmol) and formic acid (20 mL) was heated under reflux for 6 h. The reaction mixture was poured onto ice-cold water (30 mL). The resulting solid was collected and crystallized from ethanol.

Buff crystals; yield 90%; m.p.: 175–177 °C; IR (KBr, cm^{-1}): 3311 (NH), 3070 (Ar–H), 1710 (C=O chromen), 1670 (C=O amide); ^1H NMR (400 MHz, DMSO-d_6): 3.86 (s, 3H, OCH_3), 7.10 (d, 2H, J = 8 Hz, Ar–H), 7.17 (d, 2H, J = 8 Hz, Ar–H), 7.77 (s, 1H, NH, exchangeable by D_2O), 7.93 (t, 2H, Ar–H), 8.09 (s, 1H, H-Pyridine), 8.21 (s, 1H, H-chromen), 8.38 (s, 1H, H-Pyrimidine); ^{13}C NMR (100 MHz, DMSO-d_6): δ = 56.07 (OCH_3), 103.40, 115.28, 115.34, 115.68, 117.51, 124.87, 132.90, 133.57, 133.83, 150.59, 160.94, 163.03, 163.55 (2CO); MS (EI, 70 eV): m/z (%) = 397 [M^{+}] (6.13), 40 (100); Anal. calcd for $\text{C}_{23}\text{H}_{15}\text{N}_3\text{O}_4$ (397.38): C, 69.52; H, 3.80; N, 10.57; Found: C, 69.79; H, 3.67; N, 10.80%.

3-(4-Amino-5-(4-methoxyphenyl)pyrido[2,3-d]pyrimidin-7-yl)-2H-chromen-2-one (8)

A mixture of compound **2** (10 mmol) and formamide (20 mL) was heated under reflux for 20 h. The reaction mixture was cooled, and then poured onto ice-cold water (30 mL). The resulting solid was filtered and crystallized from ethanol.

Yellow oil; yield 65%; b.p.: 200–202 °C; IR (KBr, cm^{-1}): 3393 (br NH_2), 3050 (Ar–H), 1715 (C=O chromen); ^1H NMR (400 MHz, DMSO-d_6): δ = 3.84 (s, 3H, OCH_3), 6.99 (s, 2H, NH_2 , exchangeable by D_2O), 7.05–7.95 (m, 9H, ArH), 8.09 (s, 1H, H-Pyridine), 9.85 (s, 1H, H-chromen); MS (EI, 70 eV): m/z (%) = 396 [M^{+}] (5.80), 381 (100); Anal. calcd for $\text{C}_{23}\text{H}_{16}\text{N}_4\text{O}_3$ (396.40): C, 69.69; H, 4.07; N, 14.13; Found: C, 70.02; H, 4.21; N, 14.35%.

2-Amino-4-(4-methoxyphenyl)-6-(2-oxo-2H-chromen-3-yl)nicotinamide (9)

A sample of compound **2** (10 mmol) was warmed in 60% aqueous H_2SO_4 (10 mL) with stirring for 30 min. The reaction mixture was cooled, diluted with ice-cold water (20 mL) and then neutralized at PH = 8 by addition of 10% NaOH. The resulting solid was filtered and crystallized from ethanol.

Off-white crystals; yield 86%; m.p.: 250–252 °C; IR (KBr, cm^{-1}): 3417 (2 NH_2), 3050 (Ar–H), 1720–1643 (C=O chromen and C=O amide); ^1H NMR (400 MHz, DMSO-d_6): δ = 3.86 (s, 3H, OCH_3), 6.79 (s, 2H, NH_2 , exchangeable by D_2O), 6.87 (s, 2H, NH_2 , exchangeable by D_2O), 6.96–7.22 (m, 10H, Ar–H); MS (EI, 70 eV): m/z (%) = 381 [M^{+}] (5.63), 185 (100); Anal. calcd for $\text{C}_{22}\text{H}_{17}\text{N}_3\text{O}_4$ (387.39): C, 68.21; H, 4.42; N, 10.85; Found: C, 67.94; H, 4.79; N, 11.08%.

5-(4-Methoxyphenyl)-2-methyl-7-(2-oxo-2H-chromen-3-yl)pyrido[2,3-d]pyrimidin-4(3H)-one (10)

A mixture of compound **9** (10 mmol) and glacial acetic acid (20 mL) was heated under reflux for 40 h. The reaction mixture was cooled, and then poured onto ice-cold water (30 mL). The resulting solid was filtered and crystallized from benzene.

Black crystals; yield 75%; m.p.: 80–82 °C; IR (KBr, cm^{-1}): 3258 (NH), 3050 (Ar–H), 2947, 2838 (aliphatic H), 1701, 1598 (C=O chromen and C=O amide); ^1H NMR (400 MHz, DMSO-d_6): δ = 1.88 (s, 3H, CH_3), 3.86 (s, 3H, OCH_3), 4.60 (s, 2H, NH, exchangeable by D_2O), 6.76–7.49 (m, 8H, Ar–H), 8.03 (s, 1H, H-Pyridine), 8.24 (s, 1H, H-chromen); MS (EI, 70 eV): m/z (%) = 411 [M^{+}] (1.13), 97 (100); Anal. calcd for $\text{C}_{24}\text{H}_{17}\text{N}_3\text{O}_4$ (411.41): C, 70.07; H, 4.16; N, 10.21; Found: C, 70.26; H, 4.98; N, 10.81%.

***N*-(3-Cyano-4-(4-methoxyphenyl)-6-(2-oxo-2*H*-chromen-3-yl)pyridin-2-yl)acetamide (11)**

This compound was synthesized by two methods:

- A mixture of compound **2** (10 mmol) and triethylorthoformate (20 mmol) in dry acetic anhydride (20 mL) was heated under reflux for 3 h. Then, the reaction mixture was cooled, poured onto ice-cold water (30 mL). The resulting solid was collected and crystallized from ethanol.
- Compound **2** (10 mmol) was heated under reflux in acetic anhydride (20 mL) for 5 h. Then, the reaction mixture was cooled, poured onto ice-cold water (30 mL). The resulting solid was filtered, dried, and crystallized from ethanol.

Brown crystals; yield 76%, m.p.: 125–127 °C; IR (KBr, cm^{-1}): 3264 (NH), 3070 (Ar–H), 2942, 2841 (aliphatic H), 2218 (CN), 1691 (C=O chromen and C=O amide); ^1H NMR (400 MHz, DMSO-d_6): δ = 2.27 (s, 3H, COCH_3), 3.86 (s, 3H, OCH_3), 6.98 (d, 2H, J = 8 Hz, Ar–H), 7.14 (t, 2H, Ar–H), 7.33 (d, 2H, J = 8 Hz, Ar–H), 7.97 (d, 1H, J = 8 Hz, Ar–H), 8.03 (d, 1H, J = 8 Hz, Ar–H), 8.20 (s, 1H, H-Pyridine), 8.37 (m, 1H, H-chromen), 10.97 (s, 1H, NH, exchangeable by D_2O); ^{13}C NMR (100 MHz, DMSO-d_6): δ = 25.64 (CH_3), 56.19 (OCH_3), 77.33, 103.25, 115.27 (CN), 115.36, 115.46, 115.68, 116.73, 124.45, 124.58, 132.90, 133.49, 133.69, 133.82, 152.68, 160.93, 163.24, 163.70, 164.82, 172.08 (CO); MS (EI, 70 eV): m/z (%) = 411 (3.07) [M^{+}], 282 (100); Anal. calcd for $\text{C}_{24}\text{H}_{17}\text{N}_3\text{O}_4$ (411.41): C, 70.07; H, 4.16; N, 10.21; Found: C, 70.34; H, 4.35; N, 10.49%.

***N*-Acetyl-*N*-(3-cyano-4-(4-methoxyphenyl)-6-(2-oxo-2*H*-chromen-3-yl)pyridin-2-yl)acetamide (13)**

A mixture of compound **2** (10 mmol) was heated under reflux in a 1:4 mixture of acetic anhydride (5 mL) and pyridine (20 mL) at 80 °C 1 h. After cooling, the reaction mixture was poured onto ice-cold water (20 mL). The resulting precipitate thus formed was collected and crystallized from acetic acid.

Greenish white crystals; yield 76%, m.p.: 100–103 °C; IR (KBr, cm^{-1}): 3070 (Ar–H), 2940, 2841 (aliphatic H), 2215 (CN), 1691 (C=O); ^1H NMR (400 MHz, DMSO-d_6): δ = 1.89 (s, 6H, 2 COCH_3), 3.86 (s, 3H, OCH_3), 7.09 (d, 2H, J = 8 Hz, Ar–H), 7.14 (d, 2H, J = 8 Hz, Ar–H), 7.70 (t, 2H, Ar–H), 7.92 (d, 1H, J = 8 Hz, Ar–H), 8.12 (s, 1H, H-Pyridine), 8.16 (d, 1H, J = 8 Hz, Ar–H), 8.37 (s, 1H, H-chromen); ^{13}C NMR (100 MHz, DMSO-d_6): δ = 39.34 (COCH_3), 56.39 (OCH_3), 115.27 (CN), 115.68, 124.59, 124.87, 132.90, 133.83, 150.57, 160.94, 163.03, 163.57,

164.82 (2CO); MS (EI, 70 eV): m/z (%) = 453 [M^{+}] (9.18), 297 (100); Anal. calcd for $\text{C}_{26}\text{H}_{19}\text{N}_3\text{O}_5$ (453.45): C, 68.87; H, 4.22; N, 9.27; Found: C, 69.21; H, 4.39; N, 9.41%.

3-(4-(4-Methoxyphenyl)-7-methyl-5-thioxo-5,6-dihydro-1,6-naphthyridin-2-yl)-2*H*-chromen-2-one (14)

A mixture of compound **2** (10 mmol) and thioacetamide (10 mmol) in trifluoroacetic acid (5 mL) was heated under reflux for 24 h. Then, the reaction mixture was cooled, poured onto ice-cold water (30 mL). The obtained solid was collected by filtration, washed with water, dried and crystallized from ethanol.

Pale brown crystals; yield 85%, m.p.: 158–160 °C; IR (KBr, cm^{-1}): 3350 (NH), 3060 (Ar–H), 2950, 2820 (aliphatic H), 1720–1686 (br. C=O chromen and C=O amide), 1264 (CS); ^1H NMR (400 MHz, DMSO-d_6): δ = 2.65 (s, 3H, CH_3), 3.85 (s, 3H, OCH_3), 7.06–8.03 (m, 12H, Ar–H, and NH exchangeable proton); MS (EI, 70 eV): m/z (%) = 426 [M^{+}] (16.19), 274 (100); Anal. calcd for $\text{C}_{25}\text{H}_{18}\text{N}_2\text{O}_3\text{S}$ (426.49): C, 70.40; H, 4.25; N, 6.57; Found: C, 70.27; H, 4.58; N, 6.79%.

4-(4-Methoxyphenyl)-2-(2-oxo-2*H*-chromen-3-yl)-7-phenyl-1,6-naphthyridin-5(6*H*)-one (15)

A mixture of compound **2** (10 mmol) and benzoylchloride (10 mmol) in pyridine (20 mL) was heated under reflux for 6 h. Then, the reaction mixture was cooled, poured onto ice-cold water (30 mL). The resulting solid was collected and crystallized from ethanol.

Yellowish white crystals; yield 85%; m.p.: >300 °C; IR (KBr, cm^{-1}): 3456 (br NH), 3060 (Ar–H), 2964, 2870 (aliphatic H), 1721, 1646 (C=O chromen and C=O amide); ^1H NMR (400 MHz, DMSO-d_6): δ = 3.85 (s, 3H, OCH_3), 6.87 (t, 3H, Ar–H), 7.09 (d, 2H, J = 8 Hz, Ar–H), 7.27 (d, 1H, J = 8 Hz, Ar–H), 7.36 (d, 1H, J = 8 Hz, Ar–H), 7.74 (t, 2H, Ar–H), 8.34 (s, 1H, H-Pyridine), 8.55 (m, 1H, H-chromen), 10.18 (s, 1H, NH, exchangeable by D_2O); MS (EI, 70 eV): m/z (%) = 473 [M^{+}] (9.68), 313 (100); Anal. calcd for $\text{C}_{30}\text{H}_{20}\text{N}_2\text{O}_4$ (472.49): C, 76.26; H, 4.27; N, 5.93; Found: C, 76.28; H, 4.23; N, 5.77%.

3-(5-Imino-4-(4-methoxyphenyl)-6-phenyl-7-thioxo-5,6,7,8-tetrahydro-1,8-naphthyridin-2-yl)-2*H*-chromen-2-one (17)

A mixture of compound **2** (10 mmol) and phenylisothiocyanate (10 mmol) in pyridine (20 mL) was heated under reflux for 7 h. The reaction mixture was cooled, diluted with ethanol. The formed precipitate was filtered and crystallized from ethanol to afford compound 17.

Dark yellow crystals; yield 87%; m.p.: 136–138 °C; IR (KBr, cm^{-1}): 3302 (br NH), 3057 (Ar–H), 2940, 2833

(aliphatic H), 1685 (C=O chromen), 1250 (C=S); ^1H NMR (400 MHz, DMSO- d_6): δ = 3.02 (s, 1H, NH=C-CH-C=S), 3.83 (s, 3H, OCH₃), 6.51 (d, 2H, J = 8 Hz, Ar-H), 6.90 (t, 1H, Ar-H), 7.10 (d, 2H, J = 8 Hz, Ar-H), 7.25 (t, 2H, Ar-H), 7.31 (t, 2H, Ar-H), 7.39 (d, 2H, J = 8 Hz, Ar-H), 7.44 (d, 1H, J = 8 Hz, Ar-H), 7.84 (d, 2H, J = 8 Hz, Ar-H), 7.93 (d, 1H, J = 8 Hz, Ar-H), 8.56 (s, 1H, H-Pyridine), 8.63 (s, 1H, NH, exchangeable by D₂O), 9.76 (s, 1H, H-chromen); 9.85 (s, 1H, NH exchangeable by D₂O); ^{13}C NMR (100 MHz, DMSO- d_6): δ = 56.08 (OCH₃), 114.97 (CN), 115.28, 118.60, 122.23, 124.05, 124.35, 124.84, 128.86, 129.11, 129.22, 129.39, 130.01, 132.90, 139.90, 140.16, 150.05, 105.59, 152.99 (CO), 180.05 (CS); MS (EI, 70 eV): m/z (%) = 503 [M^+] (3.87), 408 (100); Anal. calcd for C₃₀H₂₁N₃O₃S (503.57): C, 71.55; H, 4.20; N, 8.34; Found: C, 71.30; H, 4.37; N, 8.62%.

3-(5-(4-Methoxyphenyl)-2,4-dithioxo-1,2,3,4-tetrahydropyrido[2,3-d]pyrimidin-7-yl)-2H-chromen-2-one (18)

To a solution of compound **2** (10 mmol) in pyridine (10 mL), carbon disulfide (50 mmol) was added and the mixture was heated under reflux on a water bath for 8 h. After cooling, ethanol was added and the resulting solid was filtered, washed with ethanol to produce the target compound **18**.

Yellow crystals; yield 80%, m.p.: 145–147 °C; IR (KBr, cm^{-1}): 3448, 3182 (2NH), 3050 (Ar-H), 2960, 2849 (aliphatic H), 1696 (C=O chromen), 1264 (CS); ^1H NMR (400 MHz, DMSO- d_6): δ = 3.83 (s, 3H, OCH₃), 7.10 (d, 2H, J = 8 Hz, Ar-H), 7.16 (d, 2H, J = 8 Hz, Ar-H), 7.64 (s, 1H, NH, exchangeable by D₂O), 7.77 (s, 1H, NH, exchangeable by D₂O), 7.93 (t, 2H, Ar-H), 8.09 (s, 1H, H-Pyridine), 8.38 (s, 1H, H-chromen); ^{13}C NMR (100 MHz, DMSO- d_6): δ = 56.08 (OCH₃), 103.40, 115.28 (CN), 117.51, 124.87, 132.90, 150.58, 163.03 (CO), 163.55 (2CS); MS (EI, 70 eV): m/z (%) = 445 [M^+] (26.96), 307 (100); Anal. calcd. for C₂₃H₁₅N₃O₃S₂ (445.51): C, 62.01; H, 3.39; N, 9.43; O; Found: C, 61.87; H, 3.52; N, 9.68%.

In vitro anti-tumor assay

Methodology: cell culture

Hepatic (HepG-2), human colon (HCT-116), breast (MCF-7), and lung (A549) cancer cell lines were obtained from the American Type Culture Collection (ATCC, Rockville, MD, USA).

The cells were grown in RPMI-1640 medium, supplemented with 10% inactivated fetal calf serum and 50 $\mu\text{g mL}^{-1}$ gentamycin. The cells were maintained at 37 °C in a humidified atmosphere with 5% CO₂.

Cell growth inhibitory assay

Viability of control and treated cells were evaluated using the MTT assay in triplicate. MTT assay is a laboratory experiment, and a standard colorimetric assay (an assay measures changes in color) for measuring cellular growth, yellow MTT [3-(4,5-dimethylthiazol-2-yl)-2,5-diphenyltetrazolium bromide, a tetrazole] was reduced to purple formazan in the mitochondria of living cells. A solubilizing solution DMSO was added to dissolve the insoluble purple formazan product into a colored solution. Briefly, four tumor cell lines were seeded in 96-well plates containing 100 μL of the growth medium at a density of 1×10^4 cells/well. Cells were permitted to adhere for 24 h till confluence, washed with PBS and then treated with different concentration of compounds in fresh maintenance medium from 50 to 1.56 μg and incubated at 37 °C for 24 h. A control of untreated cells was made in the absence of test compounds. Untreated cells used as negative control. Serial two fold dilutions of the tested compounds were added into a 96-well tissue culture plate using multichannel pipette (Eppendorf, Germany). After treatment (24 h), the culture supernatant was replaced by fresh medium. Then, the cells in each well were incubated at 37 °C with 100 μL of MTT solution (5 mg mL^{-1}) for 4 h. After the end of incubation, the MTT solution was removed, and then 100 μL of DMSO was added to each well. The absorbance was detected at 570 nm using a microplate reader (SunRise TECAN, Inc, USA). The absorbance of untreated cells was considered as 100%. The results were determined by three independent experiments (Liu et al. 1997).

Cell cycle analysis (DNA-flow cytometry analysis)

Hepatic (HepG-2), human colon (HCT-116), breast (MCF-7), and lung (A549) cancer cell lines at a density of 4×10^6 cells by T 75 flasks were exposed to compounds **9**, **10**, and **11** at their IC₅₀ for 24 h. The cells then were collected by trypsinization, washed in phosphate buffered saline and fixed in ice-cold absolute alcohol. Thereafter, cells were stained using Cycle TEST™ PLUS DNA Reagent Kit (BD Biosciences, San Jose, CA) according to the manufacturer's instructions. Cell cycle distribution was determined using a FACS Calibur flow cytometer (BD Biosciences, San Jose, CA).

Caspase-3 enzyme assay

Cells were obtained from American Type Culture Collection, and cells were grown in RPMI 1640 containing 10% fetal bovine serum at 37 °C, stimulated with the compounds to be tested for caspase 3, and lysed with Cell Extraction Buffer. This lysate was diluted in standard diluent buffer

over the range of the assay and measured for human active caspase 3 content (cells are plated in a density of $1.2\text{--}1.8 \times 10,000$ cells/well in a volume of $100 \mu\text{L}$ complete growth medium + $100 \mu\text{L}$ of the tested compound per well in a 96-well plate for 48 h before the enzyme assay).

Docking study

The docking simulation was performed using Molecular Operating Environment (MOE-Dock 2008.10) software. The structures of **9**, **10**, and **11** were constructed using the builder button. Then, these compounds were subjected to energy minimization by using the default MMFF94x force field in the MOE program. Here, the low energy 3D conformers of the tested compounds were docked into the active site of caspase-3 enzyme (PDB ID: 1GFW). The lowest energy conformation was selected and exposed to an additional energy minimization using the CHARMM force field that explores all possible chiralities and bond rotations.

Compliance with ethical standards

Conflict of interest The authors declare that they have no conflict of interest.

Publisher's note: Springer Nature remains neutral with regard to jurisdictional claims in published maps and institutional affiliations.

References

- Benci K, Mandić L, Suhina T, Sedić M, Klobučar M, Pavelić SK, Pavelić K, Wittine K, Mintas M (2012) Novel coumarin derivatives containing 1,2,4-triazole, 4,5-dicyanoimidazole and purine moieties: synthesis and evaluation of their cytostatic activity. *Molecules* 17:11010–11025. <https://doi.org/10.3390/molecules170911010>
- Blank M, Shiloh Y (2007) Programs for cell death: apoptosis is only one way to go. *Cell Cycle* 6:686–695. <https://doi.org/10.4161/cc.6.6.3990>
- Chan KT, Meng FY, Li Q, Ho CY, Lam TS, To Y, Lee WH, Li M, Ch KH, Toh M (2010) Cucurbitacin B induces apoptosis and S phase cell cycle arrest in BEL-7402 human hepatocellular carcinoma cells and is effective via oral administration. *Cancer Lett* 294:118–124. <https://doi.org/10.1016/j.canlet.2010.01.029>
- Eissa SI (2017) Synthesis, characterization and biological evaluation of some new indomethacin analogs with a colon tumor cell growth inhibitory activity. *Med Chem Res* 26:2205–2220. <https://doi.org/10.1007/s00044-017-1932-8>
- El-Gaby MSA, Abdel-Gawad SM, Ghorab MM, Heiba HI, Aly HM (2006) Synthesis and biological activity of some novel thieno [2,3-*b*]quinoline, quinolino[3',2':4,5]thieno[3,2-*d*]pyrimidine and pyrido[2',3':4,5]thieno[2,3-*b*]quinoline derivatives. *Phosphorus Sulfur Silicon Relat Elem* 181:279–297. <https://doi.org/10.1080/104265090970322>
- Fan CD, Su H, Zhao J, Zhao BX, Zhang SL, Miao JY (2010) A novel copper complex of salicylaldehyde pyrazole hydrazone induces apoptosis through upregulating integrin $\beta 4$ in H322 lung carcinoma cells. *Eur J Med Chem* 45:1438–1446. <https://doi.org/10.1016/j.ejmech.2009.12.048>
- Juliana PMG, Cássia RPC, Eliana AV, José-Manuel M, Mariana FF, Nicolás O, Iracilda Z, Wagner V (2011) Antitumoral, mutagenic and (anti)estrogenic activities of tingenone and pristimerin. *Rev Bras Farmacogn* 21:963–971. <https://doi.org/10.1590/S0102-695X2011005000153>
- Kamal A, Shaik B, Nayak VL, Nagaraju B, Kapure JS, Malik MS, Shaik TB, Prasad B (2014) Synthesis and biological evaluation of 1,2,3-triazole linked aminocombretastatin conjugates as mitochondrial mediated apoptosis inducers. *Bioorg Med Chem* 22:5155–5167. <https://doi.org/10.1016/j.bmc.2014.08.008>
- Kini SG, Choudhary S, Mubeen M (2012) Synthesis, docking study and anticancer activity of coumarin substituted derivatives of benzothiazole. *J Comput Methods Mol Des* 2:51–60
- Lee D, Long SA, Adams JL, Chan G, Vaidya KS, Francis TA, Kikly K, Winkler JD, Sung C-M, Debouck C, Richardson S, Levy MA, DeWolf WE, Keller Jr PM, Tomaszek T, Head MS, Ryan MD, Haltiwanger RC, Liang P-H, Janson CA, McDevitt PJ, Johanson K, Concha NO, Chan W, Abdel-Meguid SS, Badger AM, Lark MW, Nadeau DP, Suva LJ, Gowen M, Nuttall ME (2000) Potent and selective nonpeptide inhibitors of caspases 3 and 7 inhibit apoptosis and maintain cell functionality. *J Biol Chem* 275:16007–16014
- Liu Y, Peterson DA, Kimura H, Schubert D (1997) Mechanism of cellular 3-(4,5-dimethylthiazol-2-yl)-2,5-diphenyltetrazolium bromide (MTT) reduction. *J Neurochem* 69:581–593
- Marshall ME, Kervin K, Benefield C, Umerani A, Albainy-Jenei S, Zhao Q, Khazaeli MB (1994) Growth-inhibitory effects of coumarin (1, 2-benzopyrone) and 7-hydroxycoumarin on human malignant cell lines in vitro. *J Cancer Res Clin Oncol* 120:3–10
- Molecular Operating Environment (MOE) (2008) 10, Chemical Computing Group Inc., Montréal, Canada. <http://www.chemcomp.com>
- Musa MA, Badisa LDV, Latinwo LM, Patterson TA, Owens AM (2012) Coumarin-based benzopyranone derivatives induced apoptosis in human lung (A549) cancer cells. *Anticancer Res* 32:4271–4276
- Musa MA, Joseph MY, Latinwo LM, Badisa V, Cooperwood JS (2015) In vitro evaluation of 3-arylcoumarin derivatives in A549 cell line. *Anticancer Res* 35:653–659
- Nadia HM, Emad AD (2018) Synthesis, anticancer assessment on human breast, liver and colon, carcinoma cell lines and molecular modeling study using novel pyrazolo[4,3-*c*]pyridine derivatives. *Bioorg Chem* 77:203–214. <https://doi.org/10.1016/j.bioorg.2017.12.032>
- Nagaraju K, Parvesh S, Neil K, Raghu R, Vipani K (2017) Recent advances (2015–2016) in anticancer hybrids. *Eur J Med Chem* 142:179–212. <https://doi.org/10.1016/j.ejmech.2017.07.033>
- Nepali K, Sharma S, Sharma M, Bedi PMS, Dhar KL (2014) Rational approaches, design strategies, structure activity relationship and mechanistic insights for anticancer hybrids. *Eur J Med Chem* 77:422–487. <https://doi.org/10.1016/j.ejmech.2014.03.018>
- Paul K, Bindal S, Luxami V (2013) Synthesis of new conjugated coumarin-benzimidazole hybrids and their anticancer activity. *Bioorg Med Chem Lett* 23:3667–3672. <https://doi.org/10.1016/j.bmcl.2012.12.071>
- Reed JC (2000) Mechanisms of apoptosis. *Am J Pathol* 157:1415–1430. [https://doi.org/10.1016/S0002-9440\(10\)64779-7](https://doi.org/10.1016/S0002-9440(10)64779-7)
- Salem MA, Marzouk MI, El-Kazak AM (2016) Synthesis and characterization of some new coumarins with in vitro antitumor and antioxidant activity and high protective effects against DNA damage. *Molecules*. <https://doi.org/10.3390/molecules21020249>
- Sashidhara KV, Avula SR, Sharma K, Palnati GR, Bathula SR (2013) Discovery of coumarin–monastrol hybrid as potential antitumor tumor-specific agent. *Eur J Med Chem* 60:120–127. <https://doi.org/10.1016/j.ejmech.2012.11.044>

- Sashidhara KV, Kumar A, Kumar M, Sarkar J, Sinha S (2010) Synthesis and in vitro evaluation of novel coumarin–chalcone hybrids as potential anticancer agents. *Bioorg Med Chem Lett* 20:7205–7211. <https://doi.org/10.1016/j.bmcl.2010.10.116>
- Shen JK, Du HP, Yang M, Wang YG, Jin J (2009) Casticin induces leukemic cell death through apoptosis and mitotic catastrophe. *Ann Hematol* 88:743–752. <https://doi.org/10.1007/s00277-008-0677-3>
- Siddiqi N, Arshad F, Khan S (2009) Synthesis of some new coumarin incorporated thiazolyl symicarbazones as anticonvulsants. *Pharm Soci* 66:161–167
- Singh KR, Lange ST, Kim KK (2011) A coumarin derivative (RKS262) inhibits cell-cycle progression, causes pro-apoptotic signaling and cytotoxicity in ovarian cancer cells. *Invest New Drugs* 29:63–72. <https://doi.org/10.1007/s10637-009-9335-4>
- Vosooghi M, Rajabalian S, Sorkhi M, Badinloo M, Nakhjiri M, Negahbani AS, Asadipour A, Mahdavi MA (2010) Synthesis and cytotoxic activity of some 2-amino-4-aryl-3-cyano-7-(dimethylamino)-4*H*-chromenes. *Res Pharm Sci* 5:9–14
- Zhao P, Chen L, Li L, Wei Z, Tong B, Jia Y, Kong L, Xia Y, Dai Y (2014) SC-III3, a novel scopoletin derivative, induces cytotoxicity in hepatocellular cancer cells through oxidative DNA damage and ataxia telangiectasia-mutated nuclear protein kinase activation. *BMC Cancer* 14:987. <https://doi.org/10.1186/1471-2407-14-987>